Magnetic Anisotropy Energy and Interlayer Exchange Coupling in ultrathin ferromagnets: experiment versus theory

Klaus Baberschke

Magnetic Anisotropy Energy and Interlayer Exchange Coupling in ultrathin ferromagnets: experiment versus theory

Journal:	*Philosophical Magazine & Philosophical Magazine Letters*
Manuscript ID:	TPHM-08-May-0134.R1
Journal Selection:	Philosophical Magazine
Date Submitted by the Author:	13-Jun-2008
Complete List of Authors:	Baberschke, Klaus; Freie Universitaet Berlin
Keywords:	magnetic anisotropy, magnetic films
Keywords (user supplied):	interlayer exchange
Note: The following files were submitted by the author for peer review, but cannot be converted to PDF. You must view these files (e.g. movies) online.	
ICCMS2008.tex	

Philosophical Magazine,
Vol. 00, No. 00, DD Month 200x, 1–10

Magnetic Anisotropy Energy and Interlayer Exchange Coupling in ultrathin Ferromagnets: Experiment versus Theory

Klaus Baberschke*

Institut für Experimentalphysik, Freie Universität Berlin, Arnimallee 14, D-14195 Berlin, Germany

(June 17, 2008)

To study magnetism and crystallography of nanostructures is one of the most challenging topics, at present. Novel structures were grown, which do not exist in the bulk; the magnetism of these nano-sized particles and films may differ from the bulk by orders of magnitude. Synergistic applications of theory and experiment in materials science are all important for a fundamental understanding. Most important parameters are the Magnetic Anisotropy Energy (MAE) and the Interlayer Exchange Coupling (IEC) in multilayers. We will discuss examples where *ab initio* calculations adapted to existing experiments disentangle the importance of surface and volume effects in the MAE, as well as a layer-resolved IEC and its T-dependence. The Weinberger-group has unambiguously shown that the "volume part" of MAE is most important to understand the spin reorientation transition (SRT) in Ni/Cu. They also calculated the IEC layer-by-layer in the T=0 limit for a trilayer. Very recently, in theory, spin wave excitation were added to interpret the experimental findings.

1 Introduction

Magnetism has been a fascinating field for a long time. Traditionally two subgroups have been developed: the single particle magnetism of isolated atoms and molecules and the collective magnetism with ordering phenomena, critical temperature of an ensemble of localized or itinerant magnetic moments. Into the first category belong, for example dilute 3d, 4f ions , but also Cu, Ag, Au atoms in the gas phase, they carry a magnetic moment. In an external magnetic field H_0, they undergo the Zeeman effect, and various experimental techniques (e. g. optical spectroscopy, paramagnetic resonance, etc.) can be used to measure the orbital and spin part of the magnetic moment per particle. The second category focuses on magnetic order, ferro-, or antiferromagnetism. Here the majority of experiments is dealing with hysteresis loops, coercive fields, magnetic domains etc. In this group most of the experimental techniques are limited to temperatures $T < T_c$. Spin polarized PE, MOKE, XMCD, they all loose their signal with vanishing magnetization M. As a matter of fact, a large fraction of the literature calls the regime above T_c "nonmagnetic" instead of "paramagnetic". However both, the para- and ferromagnetic phase, carry the same fingerprint, namely orbital and spin magnetic moments, μ_L, and μ_S. μ_L and its anisotropy is the only origin of magnetic anisotropy energy (beside a dipolar contribution). In both phases, for $T \gtrless T_c$, this is manifested in the tensor components of the g-factor. In the "subgroup of ferromagnetism" various names have been introduced, like magneto-elastic, magnetostriction, magneto-crystalline anisotropy, etc; they all originate from the same source, the non-vanishing orbital magnetism. Even the so-called anisotropic exchange can be interpreted as hidden orbital magnetism, projected into spin-space. For an isotropic Heisenberg Hamiltonian, $\mathbf{S_i} \cdot \mathbf{S_j}$ it costs no energy to rotate parallel (or antiparallel) aligned spins in space. Only the orbital angular moment $\mathbf{L}$, the non-spherical charge distribution, couples to $\mathbf{r}$-space, the crystallographic lattice.

Fert and Levy [1, 2] showed, quite early, that an exchange coupling, for example of Mn-Mn pairs in a dilute Mn:Cu alloy, produce no anisotropy, the isotropic exchange interaction cannot explain the field-cooling memory in spin glasses. Only triangle coupling via an impurity, e. g. Pt or Au, creates a "missing inversion symmetry" along the Mn-Mn axis. They calculated this in 3^{rd} order perturbation theory with dominant spin-orbit interaction at the (Pt or Au) impurity site. They also pointed out, that this spin-orbit contribution is the main ingredient in the 3x3 matrix of coupling with missing inversion symmetry, i. e. the

*Corresponding author. Fax +49 30 838-55048. Email: bab@physik.fu-berlin.de

Philosophical Magazine
ISSN 1478-6435 print/ISSN 1478-6443 online © 200x Taylor & Francis
http://www.tandf.co.uk/journals
DOI: 10.1080/1478643YYxxxxxxxx

Dzyakoshinsky-Moriya interaction (DM). The DM interaction, as discussed at this conference, is the lowest order coupling with missing inversion symmetry for the off-diagonal matrix elements - a unidirectional mechanism. It did explain the memory effect in spin glasses and it will explain the exchange bias at interfaces of nanostructures, today. On todays level a 3^{rd} order perturbation theory using Schrödingers equation may not be sufficient - in some cases. One might go right away and solve the full Dirac equation. That however, means that we should not use the picture of Pauli particles, but directly the Dirac particles, with the spin not being a good quantum number. In any case, only the orbital magnetism causes anisotropy in magnetism. Without it, we would have no hard magnets and no magnetic storage media.

Most of the experiments do not measure the anisotropy field (or the interlayer exchange field), but rather the energy. That is to say, the product of $\mu \cdot \mathbf{H_{an}}$. Caution must be taken when interpreting these numbers. The magnetic moment at the surface, and at an interface differ significantly from the moment in the inner part of a nanostructure. For example, for a Co/Cu (001) film of several ML thickness, the surface layer, facing vacuum has an $\approx 32\%$ enhanced moment. But at the Co-Cu interface the Co moment is $\approx 17\%$ reduced, due to hybridization effects with Cu [3]. In this paper we will not discuss the details of the experiment, but refer to recent publications [4–8].

To calculate the MAE from *first principle* is a challenge. The difference in energy/particle in different crystallographic directions ranges from μeV to few meV, this is a small fraction out of the total energy/atom, being several eV. But, if successful, the theory has great advantage compared to experiments, it can change the crystallographic structure arbitrarily, allows to calculate the magnetism layer-by-layer, can separate orbital and spin magnetism, etc. In the following we will discuss some recent examples, in which the theory has adapted realistic experimental conditions. Both together, experiment and theory, serve for a better fundamental understanding of the MAE (Sec.2) and the IEC (Sec.3) in ferromagnetic nanostructures.

2 Magnetic Anisotropy Energy (MAE)

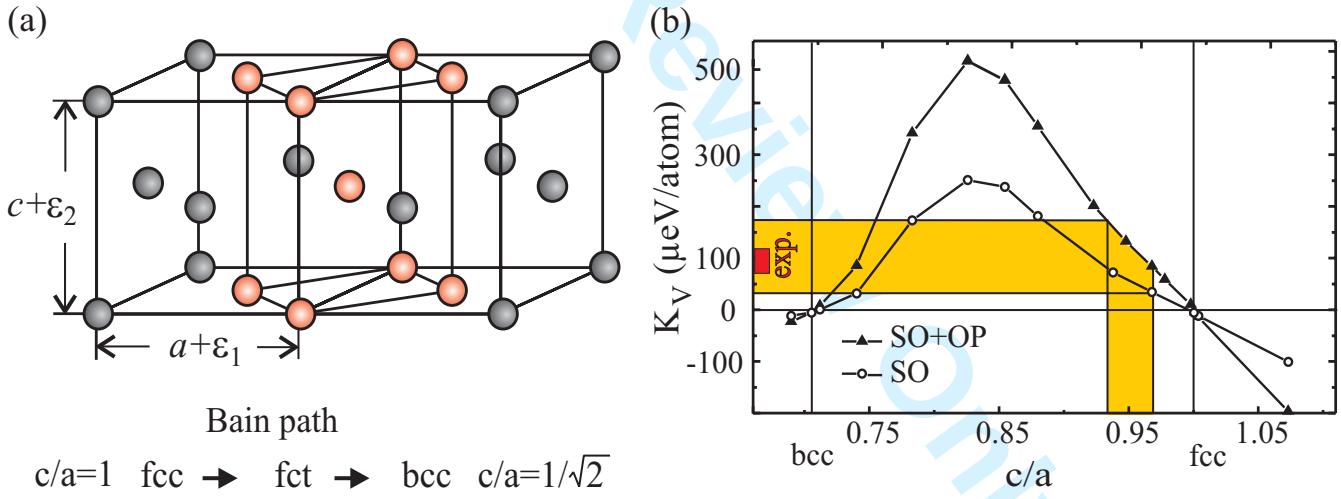

Figure 1. (color online) a) Transformation of an fcc into a bcc structure via the Bain path. b) *ab initio* calculation of K_V for an infinite-sized Ni single crystal, using spin-orbit coupling (open circles), only , and adding orbital polarization (full triangles), also. [9].

The growth of ferromagnetic ultrathin films or nanoparticles opens a complete new variety of crystallographic structures, which do not exist in the bulk. For example, tetragonal Ni can be grown epitaxially on Cu(001), or trigonal Co on Cu(111). The departure from cubic fcc structure may be small and for some aspects of electronic band structure calculations unimportant. In other words, to assume a perfect cubic lattice for Fe, Co, or Ni with the lattice constant of the Cu substrate crystal facilitates numerical calculation and may be sufficient for some aspects in the band structure and DOS, but for magnetism, the μ_L and the MAE, it is not. Already few hundreds of an $\mathring{A}$ change in the n.n. distance may change the MAE by an order of magnitude. This has been nicely demonstrated by the Uppsala theory group [9].

They assumed an infinite-sized single crystal of Ni, that is to say, no surface effects or hybridization at the interface are considered; the full MAE originates from the inner part of a crystal, the so called volume part K_V. The c/a ratio was changed from fcc with $c/a = 1$ via tetragonal symmetry to bcc with $c/a = 1/\sqrt{2}$ - the Bain path (Fig. 1a).

In experiment only one value can be realized: pseudomorphic growth of Ni/Cu(001) creates an fct structure (Fig.2a) with $c/a \approx 0.95$ with $\epsilon_1 = +2.5\%$ and $\epsilon_2 = -3.2\%$. The lateral n.n. distance in bulk Ni equals 2.49 $\AA$, on Cu(001) it is 2.55 $\AA$, a lateral stretching of 0.06 $\AA$, only! In Fig.1b we project this value of $c/a \approx 0.95$ on the theoretical SO and SO+OP calculation (yellow regime), yielding an MAE of $K_V \approx 100\mu$eV/atom, in good agreement with experiment [10]. We conclude, very small distortions in the crystal structure can change the MAE by orders of magnitude *without* employing surface effects, etc. Also in nanostructures and dots, as discussed these days, the crystal structure will depart from the bulk.

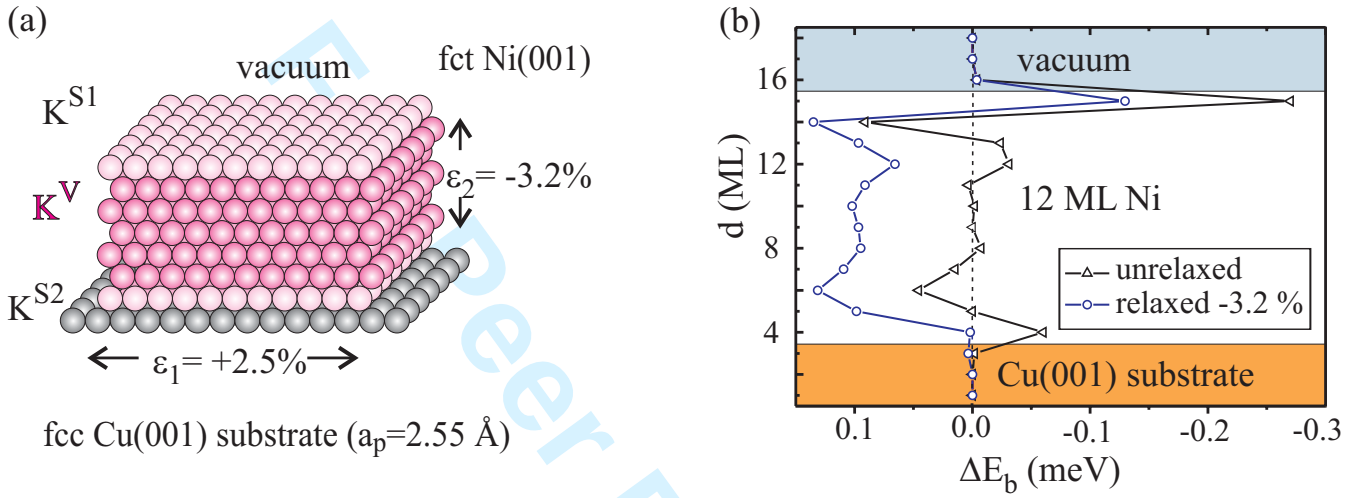

Figure 2. a) Schematic scheme of ultrathin Ni film pseudomorphically grown on Cu(001). b) *ab initio* calculation layer-by-layer of K (or ΔE_b) [11], see text.

In Fig.2a also the surface and interface contributions K_{S1} and K_{S2} to the MAE are indicated. Their contribution to the total MAE scales down with the increasing number of layers d (ML) (Néel's argument).In most experiments only the sum of the two is determined.

$$K = K_V + 2K_S/d \tag{1}$$

Here we will discuss only the intrinsic contribution K (or ΔE_b) due to the band structure. For the fct Ni crystal also a second - dipolar - contribution is calculated, but it is very small and will be neglected in the following. In experiments of ultrathin films the dipolar shape anisotropy of $2\pi M^2$ must be subtracted firstly, before discussing the K-value of Eq. (1).

The Weinberger-group has adapted the crystallographic structure of pseudomorphic Ni/Cu(001) and calculated the ΔE_b layer-by-layer for several thicknesses of the Ni films [11]. In Fig.2b we show the result for 12 ML. It is clear that the surface layer, facing vacuum, carries a large negative anisotropy energy, also the interface layer has a negative contribution. But this effects only one layer, each. The inner part of an unrelaxed (cubic) structure shows more or less no large MAE contribution. But if we accept a tetragonal distorted lattice, we see the same result as in the previous paragraph and in Fig.1: each layer contributes $+ \approx 100\mu eV$/layer (open circles in Fig.2b). We conclude: *Surface and interface contributions to the MAE may be large and negative, but count only for one layer each. The inner part of a nanostructure, K_V, will overcome this, because it counts for $n-2$ layers.*

Normally experiments cannot measure the MAE layer-by-layer, this can be extracted only from a full set of thickness dependent measurements. When varying the thickness d a second problem enters, due to the *finite size effect* also $T_C(d)$ is a function of thickness (Fig.3a). For example, to measure K and/or

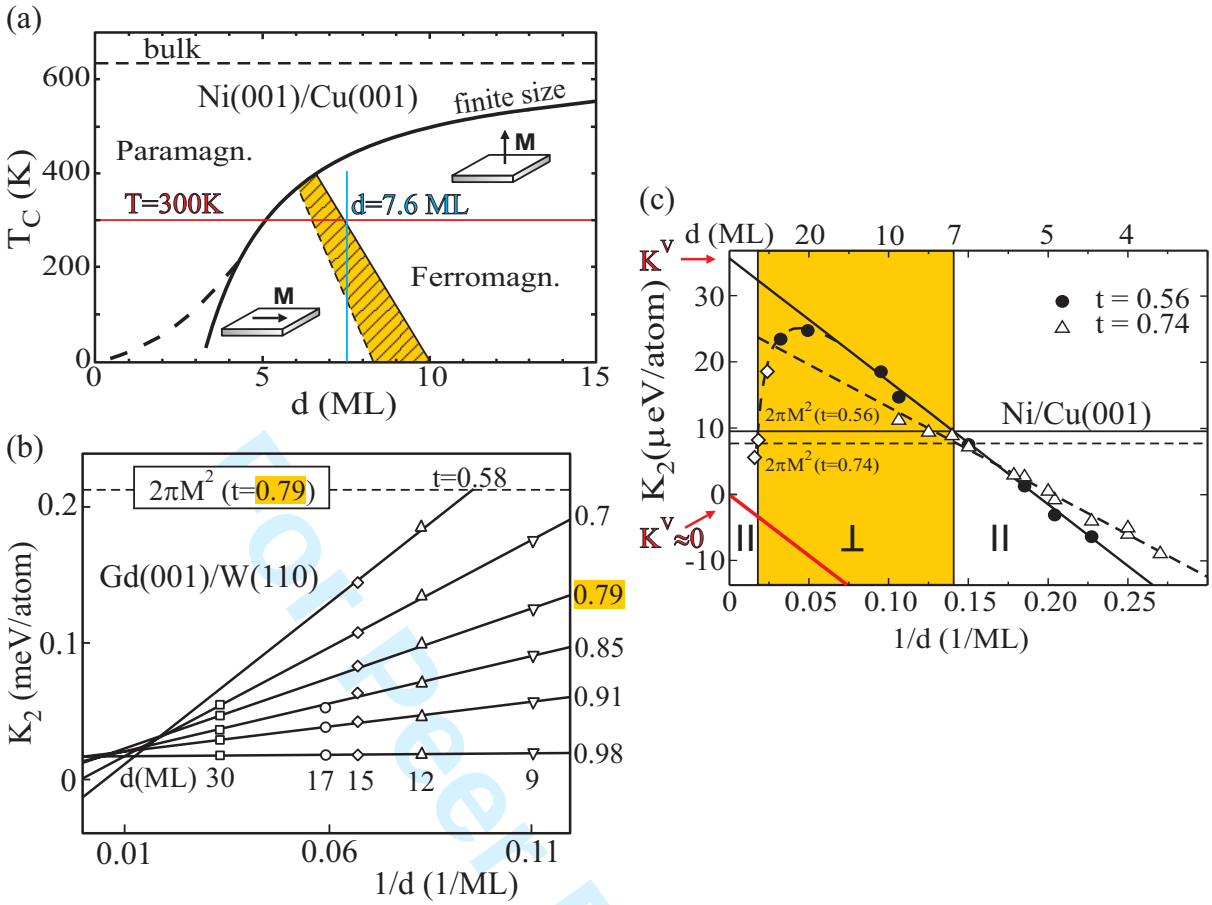

Figure 3. (color online) a) Schematic Curie temperature $T_C(d)$ for Ni/Cu(001). The solid line indicates the finite size scaling. This is an asymptotic solution for thicker films. Ultrathin films ($d =\leq 4ML$) depart from this (dashed line) and remain ferromagnetic at low T. The yellow regime indicates a continuous rotation of the easy axis from in- to out-of-plane [4]. b)Uniaxial anisotropy for Gd/W(110) as function of 1/d for different reduced temperatures [12]. c)Same plot as in b) for Ni/Cu(001)

M as $f(d)$ only at a fixed (ambient) temperature, this is of very little use, both K and M are itself a function of T, and even more complicated a function of the reduced temperature $t = T/T_C$. Both will vanish at T_C. Fig.3b demonstrates the problem: Gd films at various thicknesses were measured at different reduced temperatures [12]. With such a proper set of experimental data a reliable analysis of $K(1/d)$ may be performed. Similar results are given for Ni/Cu(001) in Fig.3c. Taking $T/T_C(d)$ into consideration, we always find a linear 1/d dependence (Eq.1). Quadratic d-dependence has been reported in the literature, that indicates changes in the crystal structure and this may produce all kinds of non-linear d and T dependences. As long as we are dealing with a given geometrical structure and want to analyze the thickness- and T-dependence of the MAE, one always expects Eq.1 to be obeyed.

Fig.3c shows the MAE as function of $1/d$ (dipole contribution is already subtracted from the experimental data). The data range from $d > 4$ML to $d < 20$ML. If normalized to the specific T_C at a given d value, the data follow obviously the linear $1/d$ dependence. All three contributions, K_V, K_S, and $2\pi M^2$ are in the range of 10 to 100 μeV/atom, that is to say, surface and volume MAE are in the same order of magnitude. Here the physics of SRT becomes very transparent: $K > 2\pi M^2$ favors out-of-plane, but if the dipolar energy wins, in-plane is the easy axis, certainly. So, let's ask the question, why happens a SRT for Ni , but not for Fe and Co? We see in Fig.3c that the dipolar contribution increases quadratic with M, i.e. for Fe and Co the horizontal $2\pi M^2$ line moves up by a factor of 8 to 14 and will never intercept with Eq.1. So, the small magnetic moment of Ni keeps the shape anisotropy low and the positive K-anisotropy may overcome this. Secondly, what causes the SRT, K_V or K_S ? Commonly it is argued in the literature, that the surface contribution is responsible. Here we show, that this is not the case: K_S is negative with a negative slope of $100 - 200\mu$eV/atom, like for many other systems (see next paragraph). But important is the intercept of $K(1/d)$ at the y-axis. For bulk fcc Ni $K_V \approx 0$ (red line) and K would never exceed $2\pi M^2$,

assuming the same negative slope . Only the large intercept of $K_V \approx 35\mu$eV/atom for the perturbed fct structure moves the linear 1/d dependence up and causes an SRT transition between 7 to 10 ML. Finally, we see at $\approx 20ML$ the experimental data depart from Eq. 1. At this thickness the Ni film "remembers " its bulk fcc structure and the crystal relaxes back to cubic symmetry with a reduced MAE and many misfit dislocations.

Ultrathin Co films on Cu have been investigated by many groups with high intensity. In the beginning of the nineties the Philips group as well as Gradmann and coworkers measured the uniaxial anisotropy K_2 of Co/Cu(111), shown as diamonds and squares in Fig.4a [13, 14]. At first glance it looks, as if K_2 increases as function of $1/d$ with a positive slope. But these data were taken at fixed (ambient) temperature and the thickness dependence of T_C was ignored. Farle et al. [15] remeasured and plotted the MAE at constant reduced temperature in Fig.4b. For ultrathin thickness of $d \leq 6$ML we see a linear $1/d$ dependence. In this regime the Co layers grow pseudomorphically on Cu(111). This produces a small trigonal ($a = b = c$ but $\alpha = \beta = \gamma \neq \pi/2$) distortion in the cubic lattice. If this perturbed cubic structure would grow up to infinite thickness, the intercept at the y-axis is about $K_V \approx 95\mu$eV/atom. This is very close to the bulk value for hcp Co. In reality the pseudomorphic growth stops at about 6 ML and we turn back to the standard fcc Co with small MAE. The arrows in Fig.4a indicate, that the data measured at 300 K will move down to negative values, when taking the change of $T_C(d)$ into account. In summary: *To the best of our knowledge, we find in the literature always $K(d)$ data following Eq.1. Furthermore we believe, that this type of "K-analysis" is one of the most sensitive techniques to detect small structural changes. It may be more sensitive than LEED or XRD*. If other thickness dependent behavior for the MAE is reported (for example quadratic, see e. g. [16]) this will be caused by structural changes as function of d or T. But then, all kinds of functional dependencies may happen, even discontinuities.

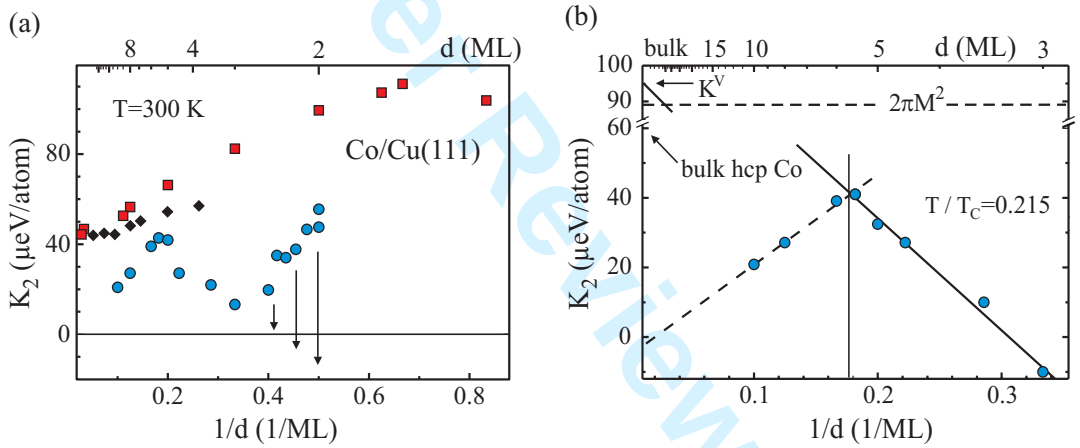

Figure 4. (color online) Uniaxial anisotropy for Co/Cu(111) as function of $1/d$, a) for a fixed temperature of $T = 300K$ and b) for a constant reduced temperature. Squares and diamonds are taken from [13, 14] and circles from [12].

Finally, we want to discuss the combined effort of theory and experiment to understand the manipulation of the surface anisotropy K_S. The Ni/Cu(001) system has been investigated by several groups, it was exposed to H, O, or CO gas [17, 18]. These authors reported a shift in the SRT moving from $\approx$ 11ML to thinner values of about 7 ML, depending on the gas adsorption. In [19] the Ni film was measured , facing vacuum, being caped with Cu, and being grown with oxygen as surfactant. The experimental results are shown in the inset of Fig.5. K_2 follows the linear 1/d dependence in the range of 5 to 12MLs with different slopes. That is not surprising, we expect only a change of the surface contribution, and indeed all 3 lines can be extrapolated to the same intercept at the y-axis of $K_V \approx$20 to 25 μeV/atom. We also see that the reduction of K_S is moderate for Cu capping, and the strongest for oxygen surfactant growth. That is explained by Wu and coworker [19] and displayed in Fig.5. They calculated the magnetic anisotropy energy for clean Ni_n slabs with both sides vacuum, for $Cu/Ni_n/Cu$ superlattices, and for a $c(2x2)$ oxygen adlayer on Ni_n films. n ranges from 5 to 15 layers. For the oxygen surfactant growth the self consistent calculation results in an outward relaxation of the top Ni layer, and a buckling of the second layer. In principle, this was known from the early research of the Ni surface, but here also the MAE of this layer was

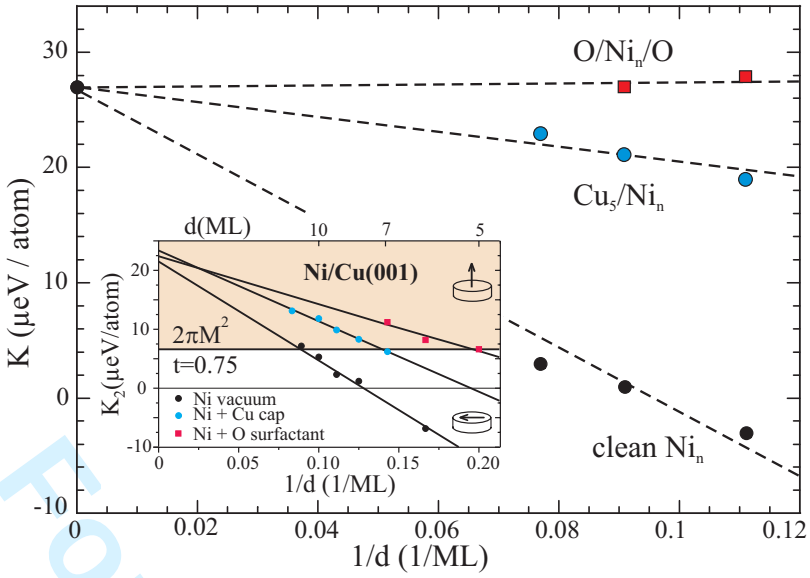

Figure 5. (color online) Calculated MAE for clean Ni films, Cu/Ni/Cu superlattices, and Ni films with a c(2x2) oxygen adlayer [19]. The inset shows the corresponding experiments. For details see text.

calculated and it turned out to be almost zero, $K_{S1} \approx 0$. Such a calculation gives also a detailed insight in the electronic band structure and how this is effected by oxygen. There is almost no change in the number of d electrons in the surface layer, there is no formation of NiO on the surface, but one finds a pronounced antibonding O-Ni peak on top of the Ni d band, i. e. an O-induced surface state with d_{xz} character. Its SO splitting is the main feature which reduces K_{S1}. This combined experimental and theoretical effect, first of all, results in a fairly good agreement. Secondly and more important, the calculated spin dependent electronic band structure can explain, what causes what.

3 Interlayer Exchange Coupling (IEC) and its temperature dependence

The second, equally important, magnetic parameter in ultrathin multilayers is the IEC. This interaction is known to oscillate between ferro- and antiferromagnetic alignment of two ferromagnetic layers, separated by a nonmagnetic spacer. A vast number of review papers are available, we refer to Chapters in [8]. When measuring or calculating the free energy, both, the MAE and the IEC, enter and it is not always easy to disentangle these. The experimental procedure in FMR measurements opens one way to determine the MAE (K) and IEC (J_{inter}), separately. In an *in situ* UHV-FMR experiment firstly a single film is measured, and the K-value determined, then the second FM film is evaporated and the only leftover parameter to be determined is J_{inter}, for details see Ref. [7]. Usually this is measured at finite temperatures and needs to be extrapolated to $T = 0$, when comparing with *ab initio* calculations .

Again, the Weinberger-group has adapted a realistic experimental situation and calculated K^j and ${J_{\text{inter}}}^j$ layer-by-layer for a prototype system of a $\text{Ni}_8/\text{Cu}_j/\text{Ni}_9$ trilayer [20]. The results are shown in Fig.6. The K-values are different for 8 and 9 ML of Ni (Fig.6 a and c) and strongly positive when the relaxation of -3.2% is taken into account (see Section 2). In Fig.6 b and d the IEC per layer is plotted. First of all, we see that for 3 ML of Cu the IEC is negative (AFM coupling) and positive (FM coupling) for 9 ML; in agreement with experiment. The main contribution to the IEC originates from the first Ni layer at the Ni/Cu interface, but also the adjacent Cu layers contribute - see Fig.6 b. We recall that at a Ni/Cu interface Cu carries an induced magnetic moment. Both, Ni and Cu, have small but finite orbital moments. This μ_L is the source, which couples - via SO interaction - the spin to the crystallographic lattice - we will come back to this. The absolute value of the calculated IEC of approximately 40 to 150 μeV is difficult to be compared to the experiment, because also the measured value is model dependent. In the analysis of the FMR data a "macroscopic" Heisenberg Hamiltonian is used, and that J_{inter} is not the same as a "microscopically" layer wise calculated IEC in Ref. [20].

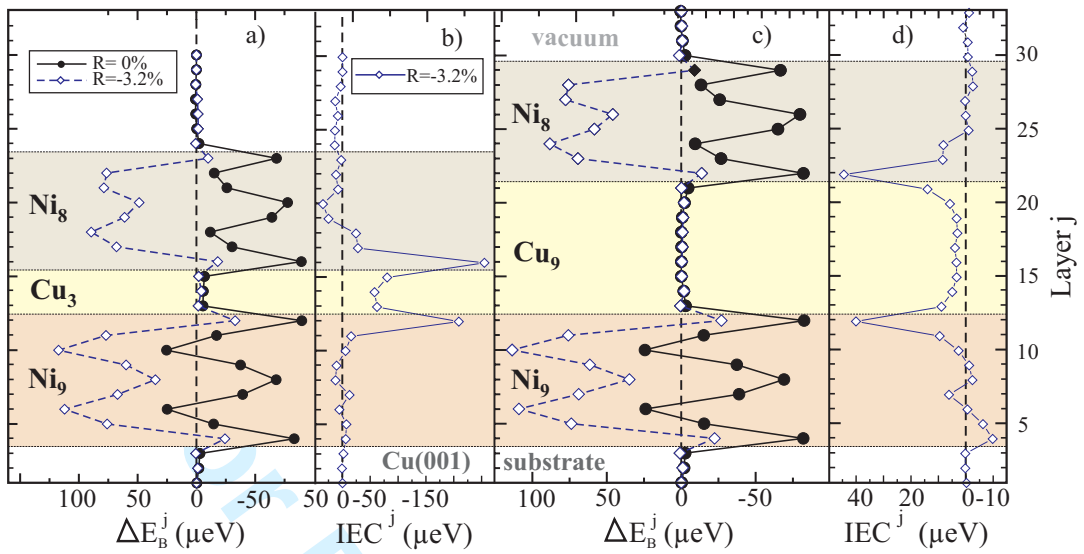

Figure 6. (color online) Calculated layer-resolved MAE (or ΔE_b) and IEC for a Ni/Cu/Ni trilayer pseudomorphically grown on a Cu(001) substrate. The number of the Ni layers is fixed to $j = 8$ and 9. The Cu spacer thickness equals $j = 3$ in a) and b) and $j = 9$ in c) and d). Taken from [20].

In earlier review articles $T = 0$ calculations have been compared with experiments measured, let's say, at room temperature. That may be justified for thicker Fe and Co films, having almost bulk T_C. For ultrathin films and in particular for Ni one needs to ask the question: What causes the T-dependence of the IEC, is it mainly an electronic band structure effect, smearing of the Fermi edge, or are spin wave excitations more important, which depend on T_C? Both theoretical models have been proposed. In Ref. [21] electronic band structure effects are investigated , leading to a T/sinh(T) functional dependence. In Ref. [22] magnetic excitations (thermal spin waves) have been discussed as the main source of the T-dependence of J_{inter}. This leads to a power law in reduced temperature T/T_C with a 3/2 exponent. On the other hand, B. Heinrich recently discusses some experiments [23] and favors a linear T-dependence. To discriminate between this various analytical functions, experimental data over a large range in temperature are needed. But which T-range is relevant? The absolute range in degree Kelvin [23] is less relevant. More important seems to

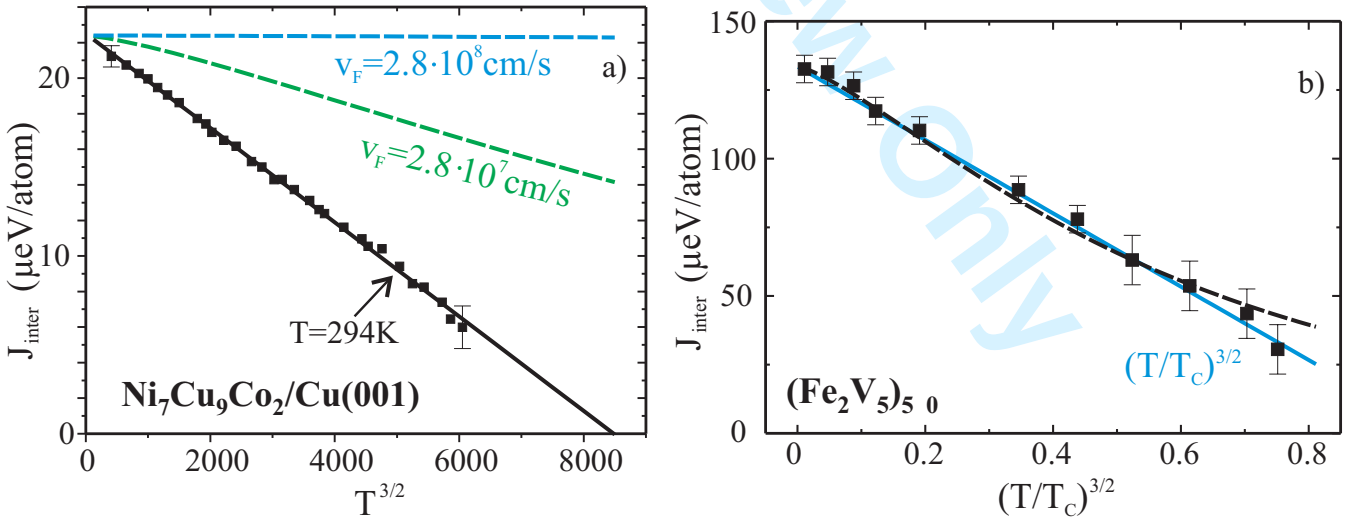

Figure 7. (color online) J_{inter} as function of temperature. In a) the trilayer was measured to $\approx$ 400K, close to T_C. In b) the data for the multilayer are shown as function of the reduced temperature t. Taken from [25].

us the reduced temperature range, that is to say, to measure from low temperatures up to T_C. And this

is difficult for several ML of Fe and Co. With the highest temperature of $400K$ for thicker Fe films [24], $t = T/T_C$ will be ≤ 0.4. We know only about one experiment [25] in which more or less the full range of reduced temperature was used. These authors measured 3 different multi- and trilayer systems (Ni/Cu/Co, Ni/Cu/Ni, and an Fe/V multilayer). The reduced temperature covers almost the total range of $0 < t \leq 0.9$, (Fig.7). Both cases, Fig.6 a and b, show an almost perfect power law behavior with a 3/2 exponent. The dashed lines are a simulation of Ref. [21] with different Fermi velocities, the same is shown in b) with the dashed line. In a more extensive calculation of the band structure effects one should try to use more than one Fermi vector and other details of the Fermi surface. The results in Fig.7 are suggesting that the spin wave excitations [22] are dominant.

Nolting and coworkers [26] discussed the electronic effects of the T-dependence in the frame of *ab initio* theory combined with Fermi liquid model, as well as in the quantum well picture. To treat collective magnetic excitations they used a microscopic Heisenberg model. In addition to the IEC, J_{inter}, also a J_{intra} is important. This is the exchange coupling within one FM film, a measure also for T_C. Its realistic values range in the meV regime, whereas J_{inter} scales in the μeV regime. To extract the effect of the magnetic contributions alone for different spacer thicknesses, J_{inter} has to be normalized to the parameter $J_0 \equiv J_{\text{inter}}(T = 0)$. This is shown in Fig.8 a and b. In a) J_0 is constant and weaker or stronger J_{intra} are used. In b) J_{intra} is kept constant, but a gentile J_0 with FM and AFM coupling is used. In all cases the authors of Ref. [26] came to the conclusion, that $J_{\text{inter}}(T)$ does not follow an exact 3/2 power law - see Fig.8 a and b. But one may want to describe the temperature dependence of the IEC with an "effective" power law with

$$J(T) \approx 1 - AT^n, \quad n \approx 1.5 \tag{2}$$

With this combined theoretical and experimental effect it seems to be evident - and also plausible - that spin wave excitations are the dominant effect for the effective reduction of the IEC at finite T. Theory has the advantage to switch on and off different mechanisms. That is shown in Fig.8, the dashed line shows the reduction of J_{inter} by spacer effects only, and the full line with "spacer + spin waves" [27].

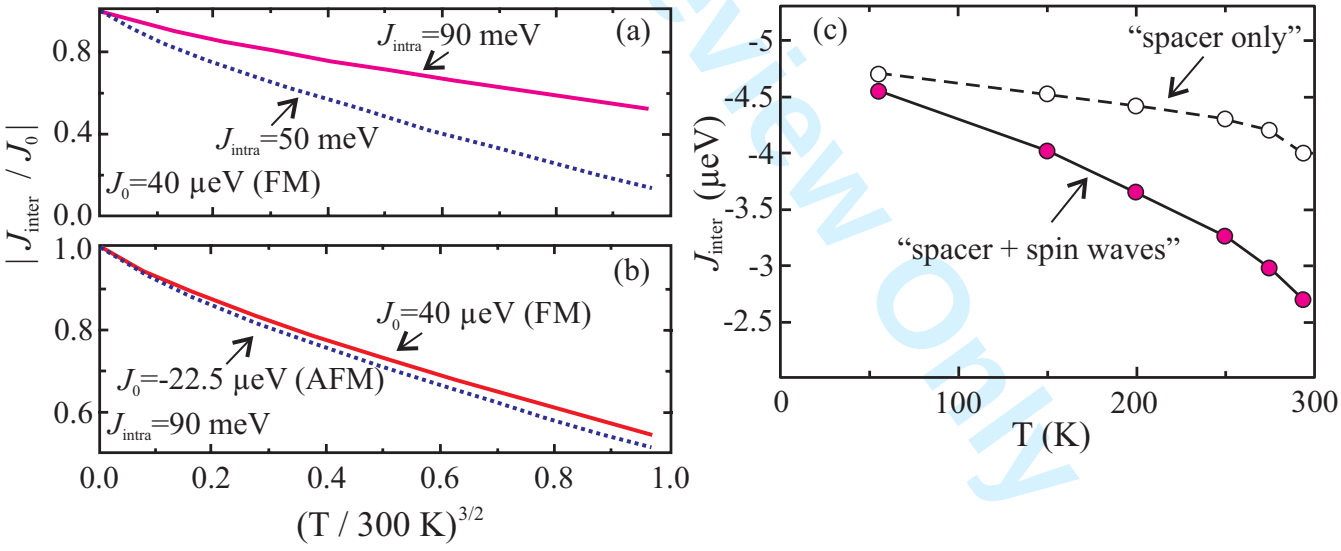

Figure 8. (color online) J_{inter}/J_0 vs. $T^{3/2}$ for a fixed J_0 in a) and for fixed J_{intra} in b), from [26]. c) shows J_{inter} as function of T, calculated with and without spin wave excitation [27].

That recent theoretical investigation in turn, inspired new FMR experiments [28]. The purpose was, to keep the two FM films constant and change only the spacer thickness n, and observe J_{inter} as function of n, that should enter into the prefactor A in Eq.2. What would we expect?

There are 3 possibilities:

1.A depends only on the interface $\Rightarrow A(d) = \text{const}$

2.A depends on electronic band structure $\Rightarrow A(d) = \text{linear fct.}$

3.A depends on spin waves, $\Rightarrow J_{\text{inter}} \Rightarrow A(d) \approx \text{osc. fct.}$

To solve the question, the Co/Cu/Ni system, with 1.8 ML Co, n monolayers of Cu spacer, and 7 ML Ni on a Cu (001) substrate was chosen [28]. This work provides for the first time an investigation of the temperature dependence of J_{inter} entirely determined from the FMR angular dependence of the ferromagnetic resonance positions at each temperature for the $n = 6$ML film (Fig.9a). Obviously, the data do not follow a monotonic function of d, i. e. the slope A for n=4 fits between n=5 and n=6. The trend in Fig.9b is clear: Large J_0 produces a weak slope A and vice versa, a very plausible result: *The IEC and the thermal energy kT are in competition. Very weak* J_{inter} *allows easily thermal excitation of spin wave, and a stronger* J_{inter} *reduces this effect.*

Real interfaces will have steps and other imperfections. For magnetic and nonmagnetic ions at these sites the local DOS will be different from the bulk., i. e. μ_S may change, but more important μ_L will increase (see Sec.2). For a given geometrical arrangement and the corresponding interplay of μ_S and μ_L this will produce a unidirectional coupling, for example between a FM and AFM film. Such unidirectional coupling leads to, what is called "exchange bias". The 3x3 matrix of $J_{\text{inter}}{}^{ij}$ may have no inversion symmetry, as discussed in [1, 2]. Indeed the DM mechanism is employed again to explain "unidirectional exchange coupling" at interfaces.

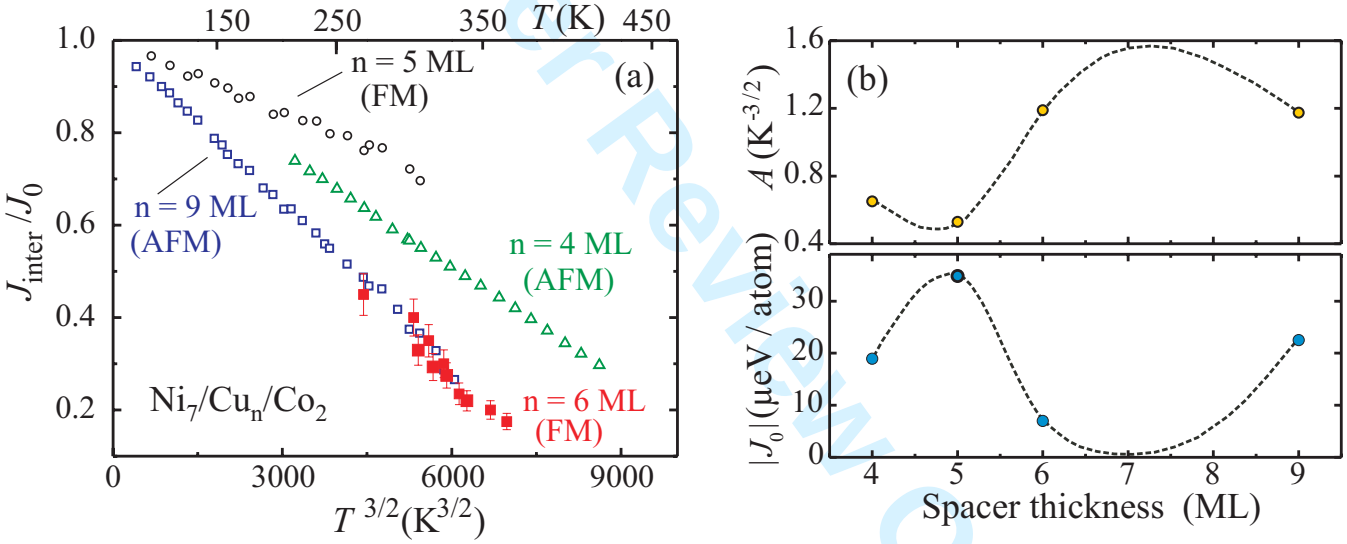

Figure 9. (color online) Normalized J_{inter} vs. $T^{1.5}$ for different spacer thickness n. The data points for the thicknesses of 4, 5 and 9 ML were taken from Schwieger *et al.*, [27], for details see [28].

4 Conclusions

Today's research on nanomagnetism, storage media, spin injection, etc. is very rich and successful. Many of the experimental findings are interpreted in a simple "'spin-up, spin-down"' picture, a common procedure in photo emission. The present contribution puts some emphasis on the fact that the orbital magnetic moment and angular momentum are crucial, they are not quenched, they originate the MAE. The anisotropy of μ_L is the leading ingredient to create an hysteresis loop with coercitive fields. Strictly speaking, not S but J is a good quantum number. In the past that has been demonstrated for Rare Earth spin glasses [29], simulating Ising or XY-systems. In some cases the 3x3 coupling matrix between two angular momentums

has lower symmetry than uniaxial. This unidirectional mechanism with missing inversion symmetry, the DM interaction, is applicable to explain the "exchange bias" and it was successful to interpret the field cooling memory effect in spin glasses [1,2]. Finally, we show that for a joined interpretation by theory and experiment in nanomagnetism one must either extrapolate the experimental observables back to $T = 0$, or include $T \neq 0$ in theory. In that case electronic band structure effects, smearing at the Fermi edge, seems to be a minor effect; most important are spin wave excitations and magnon-magnon scattering [30]. In Sec.2 we discussed the MAE and importance of orbital magnetism, in Sec.3 thermal spin wave excitations were added to understand $J_{\mathrm{inter}}(\mathrm{T})$. Both steps are more or less "static arguments". For a real detailed microscopic understanding we need to consider in addition, that magnon-magnon scattering, spin-spin correlations are all important at interfaces of ultrathin ferromagnets. Some experiments and theoretical aspects, that not the static mean field picture but higher order spin correlations control nanomagnetism, are discussed in [31, 32].

5 Acknowledgments

We are very thankful to the theorists, who picked up our experimental findings and helped so for a more fundamental understanding of MAE and IEC in ultrathin ferromagnets. These are the groups of P. Weinberger, O. Eriksson and B. Johansson, D.L. Mills and R. Wu, K.-H. Bennemann and W. Nolting. All the experiments would not have been possible without my former coworkers: J. Lindner, K. Lenz, S. S. Kalarickal, E. Kosubek, X. Xu. In particular E. Kosubek and K. Lenz are acknowledged for assistance in preparing this manuscript. This work was supported in part by BMBF (05KS4 KEB/5) and DFG Sfb 658.

References

[1] A. Fert, Peter Levy, Phys. Rev. Lett. **44**, 1538 (1980).
[2] Peter Levy, A. Fert, Phys. Rev. B **23**, 4667 (1981)
[3] A. Ney, P. Poulopoulos and K. Baberschke Europhys. Lett. **54**, 820 (2001)
[4] M. Farle, B. Mirwald-Schulz, A. Anisimov, W. Platow, and K. Baberschke Phys. Rev. B **55**, 3708 (1997)
[5] K. Baberschke, M. Farle J. Appl. Phys. **81**, 5038 (1997)
[6] A.N. Anisimov, M. Farle, P. Poulopoulos, W. Platow, K. Baberschke, P. Isberg, R. Wäppling, A.M.N. Niklasson and O. Eriksson Phys. Rev. Lett. **82**, 2390 (1999)
[7] J. Lindner and K. Baberschke, J. Phys.: Condens. Matter **15**, R193 and S465 (2003)
[8] *Handbook of Magnetism and Advanced Magnetic Materials*, K. Baberschke in Volume **3**, p.1617 Edited by Helmut Kronmüller and Stuart Parkin, 2007 John Wiley & Sons,
[9] O. Hjortstam, K. Baberschke, J.M. Wills, B. Johansson, and O. Eriksson Phys. Rev. B **55**, 15026 (1997)
[10] B. Schulz and K. Baberschke, Phys. Rev. B **50**, 13 467 (1994)
[11] C. Uiberacker, J. Zabloudil, P. Weinberger, L. Szunyogh, C. Sommers, Phys. Rev. Lett. **82**, 1289 (1999). Note that the relaxation of -5.5% in this paper is normalized to Ni and identical to -3.2% normalized to Cu in the present work.
[12] M. Farle, Rep. Prog. Physics **61**, 755 (1998)
[13] J. Kohlhepp, H.J. Elmers, U. Gradmann, J. Magn. Magn. Mater. **121**,487 (1993)
[14] F.J.A. den Broeder, W. Hoving, P.J.H. Bloemen, J. Magn. Magn. Mater. **191**,562 (1991)
[15] M. Farle, W. Platow, E. Kosubek, K. Baberschke, Surf. Sci. **439**,146 (1999)
[16] C.A.F. Vaz, J.A.C. Bland, G. Lauhoff, Rep. Prog. Phys.**71**,56501 (2008)
[17] R. Vollmer, Th. Gutjahr-Loser, J. Kirschner, S. von Dijken, B. Poelsma Phys. Rev. B **60**, 6277 (1999)
[18] S. van Dijken, R. Vollmer, B. Poelsma, J. Kirschner J. Magn. Magn. Mater. **210**,316 (2000)
[19] Jisang Hong, R.Q. Wu, J. Lindner, E. Kosubek, and K. Baberschke, Phys. Rev. Lett. **92**, 147202 (2004)
[20] R. Hammerling, J. Zabloudil, P. Weinberger, J. Lindner, E. Kosubek, R. Nünthel, and K. Baberschke, Phys. Rev. B **68**, 092406 (2003).
[21] P. Bruno, Phys. Rev. B **52**, 411 (1995) and V. Drchal, J. Kudrnovsky, P. Bruno, I. Turek, P. H. Dederichs, P. Weinberger, Phys. Rev. B **60**, 9588 (1999).
[22] N. S. Almeida, D. L. Mills, and M. Teitelman, Phys. Rev. Lett. **75**, 733 (1995).
[23] B. Heinrich in*Magnetic Heterostructures* Edited by H. Zabel and S.D. Bader, Springer Tracts of Modern Physics **227**, 185 (2008).
[24] Z. Celisnki, B. Heinrich, J.F. Cochran, J. Magn. Magn. Mater. **145**, L1 (1995)
[25] J. Lindner, C. Rüdt, E. Kosubek, P. Poulopoulos, K. Baberschke, P. Blomquist, R. Wäppling, and D. L. Mills, Phys. Rev. Lett. **88**, 167206 (2002).
[26] S. Schwieger, W. Nolting, Phys. Rev. B **69**, 224413 (2004)
[27] S. Schwieger, J. Kienert, K. Lenz, J. Lindner, K. Baberschke, and W. Nolting, Phys. Rev. Lett. **98**, 057205 (2007) and J. Magn. Magn. Mater. **310**, 2301 (2007).
[28] S. S. Kalarickal, X. Xu, K. Lenz, W. Kuch, K. Baberschke, Phys. Rev. B **75**, 224429 (2007).
[29] K. Baberschke, P. Pureur, A. Fert, R. Wendler, S. Senoussi, Phys. Rev. B **29**, 4999 (1984)
[30] J. Lindner, K. Lenz, E. Kosubek, K. Baberschke, D. Spoddig, R. Meckenstock, J. Pelzl, Z. Frait and D.L. Mills, Phys. Rev. B **68**, 060102(R) (2003).
[31] K. Baberschke, Physica status solidi (b) **245**, 174 (2008).
[32] L. Bergqvist, O. Eriksson , J. Phys.: Cond. Matter **18**, 4853 (2006)

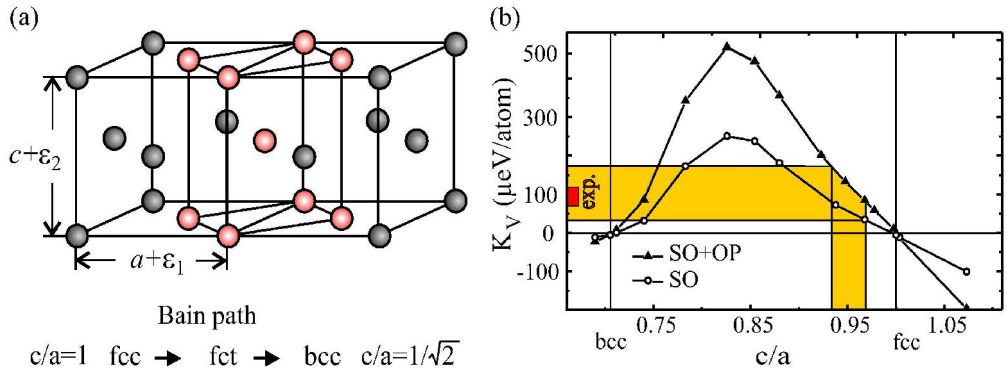

117x43mm (600 x 600 DPI)

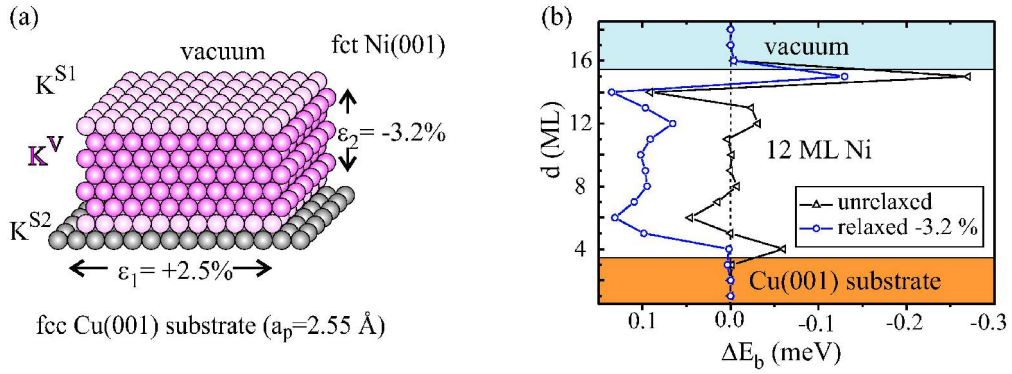

117x45mm (600 x 600 DPI)

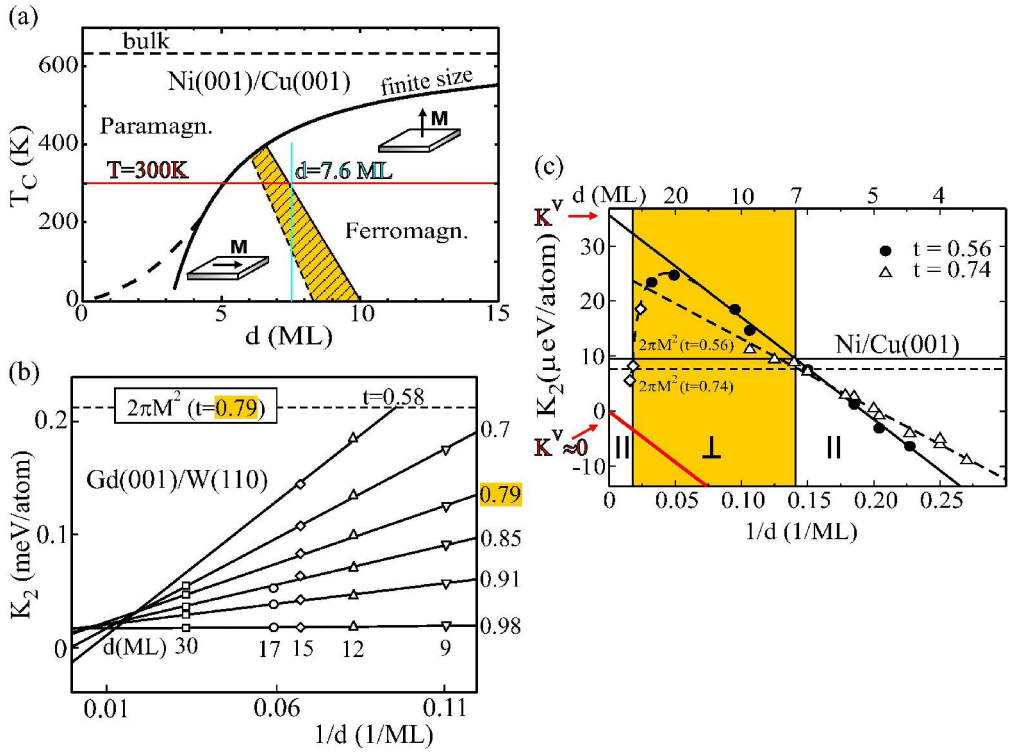

117x88mm (600 x 600 DPI)

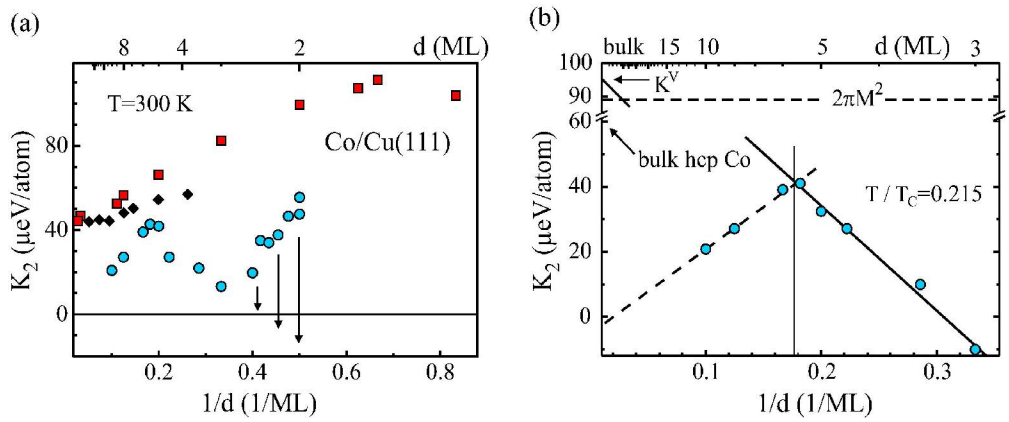

118x49mm (600 x 600 DPI)

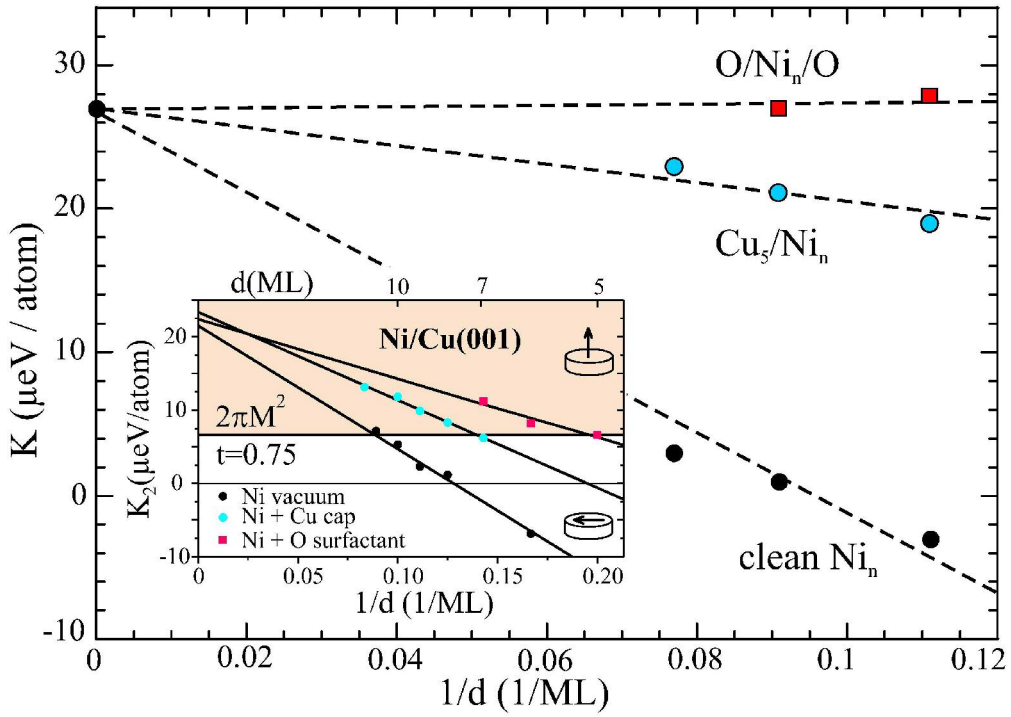

116x83mm (600 x 600 DPI)

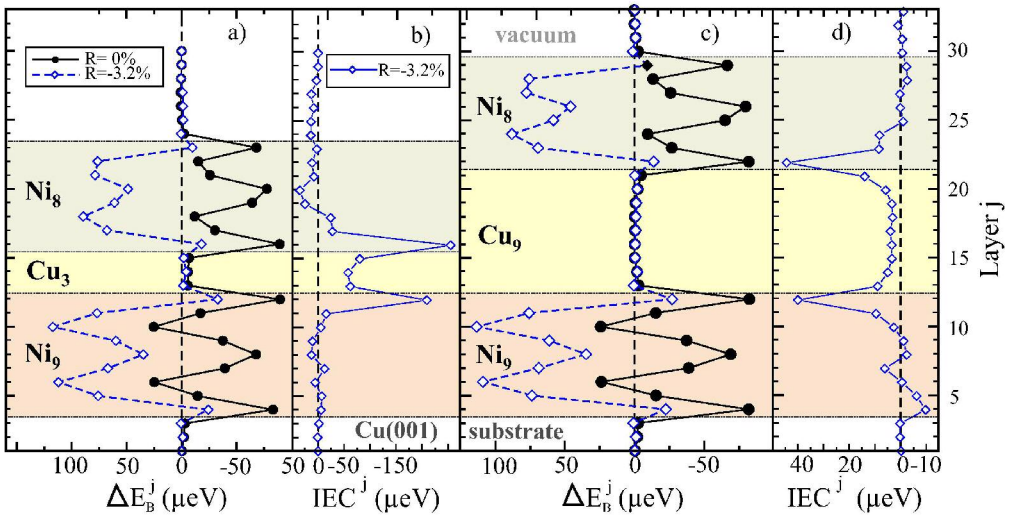

116x71mm (600 x 600 DPI)

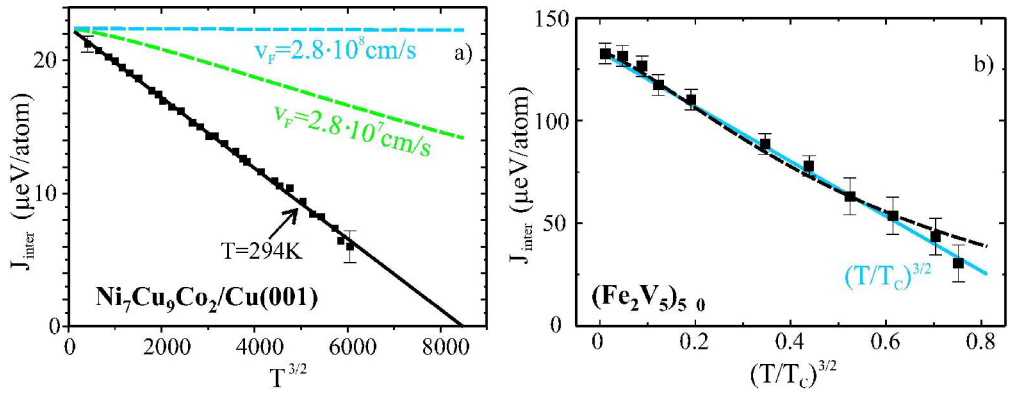

117x44mm (600 x 600 DPI)

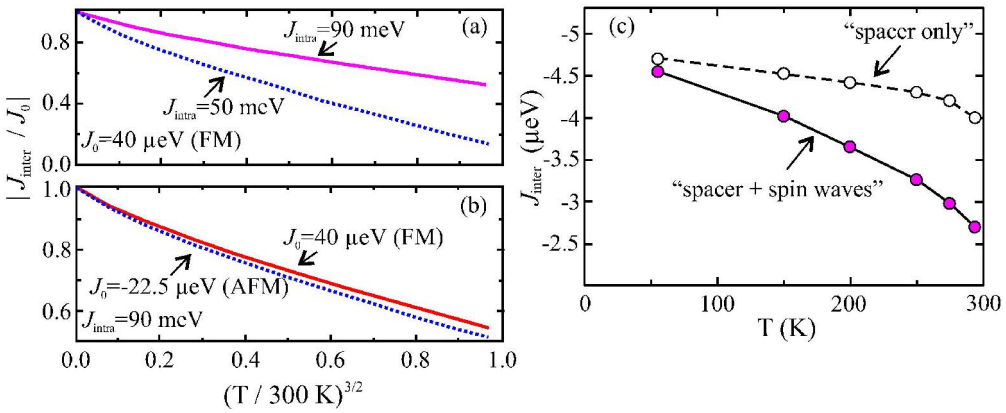

119x48mm (600 x 600 DPI)

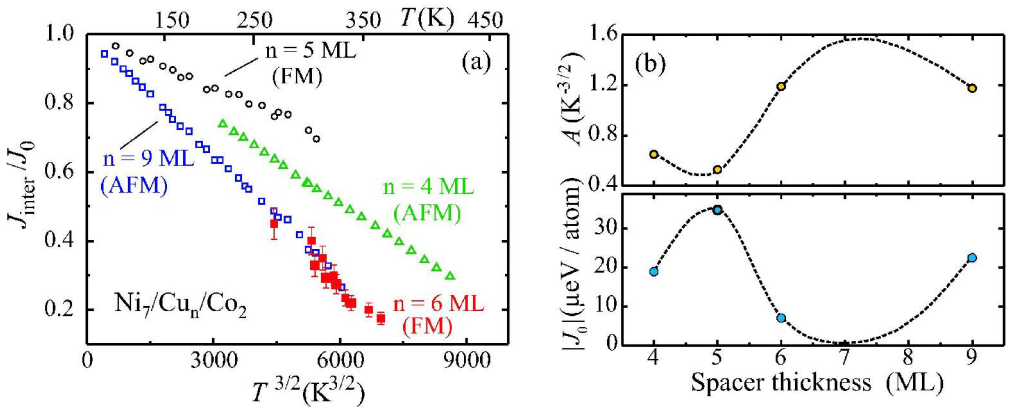

117x47mm (600 x 600 DPI)